EXPRESS LETTER

Two independent signals detected by ocean bottom electromagnetometers during a non-eruptive volcanic event: Ogasawara Island arc volcano, Nishinoshima

Kiyoshi Baba[1*], Noriko Tada[1,2], Hiroshi Ichihara[3], Yozo Hamano[4], Hiroko Sugioka[2,5], Takao Koyama[1], Akimichi Takagi[6] and Minoru Takeo[1]

Abstract

Nishinoshima is an active oceanic island arc volcano situated approximately 1000 km south of Tokyo, Japan. Since 2016, marine electromagnetic observations using ocean bottom electromagnetometers have been conducted around the island to investigate the electrical structure beneath the volcano for the first time. In contrast to the original purpose of the experiment, the data collected at five sites deployed in 2016–2017 showed distinct time variations in the magnetic field and the tilt of the volcano's slope. These time variations occurred coincidentally in mid-November 2016; this was during a quiet period between eruptions in 2015 and in 2017. The independence between the observed total magnetic force and tilt data was verified, highlighting that these variations were not artificial rather, associated with volcanic activity that did not invoke an eruption. Sources for demagnetization and deflation were estimated beneath the volcanic slope in the northeast of Nishinoshima Island, assuming a magnetic dipole and a spherical volume change, respectively. The resultant dipole moment and the volume change were too large to maintain simple source assumptions. However, the limited available data only enabled quantitative discussion under simple model settings, suggesting that the source mechanisms were more complex. The observations from this study demonstrate that if deployed strategically, ocean bottom electromagnetometers are useful to monitor island volcano activities.

Keywords: Nishinoshima, Oceanic island arc volcano, Ocean bottom electromagnetometer, Total magnetic force, Volcanic edifice deformation
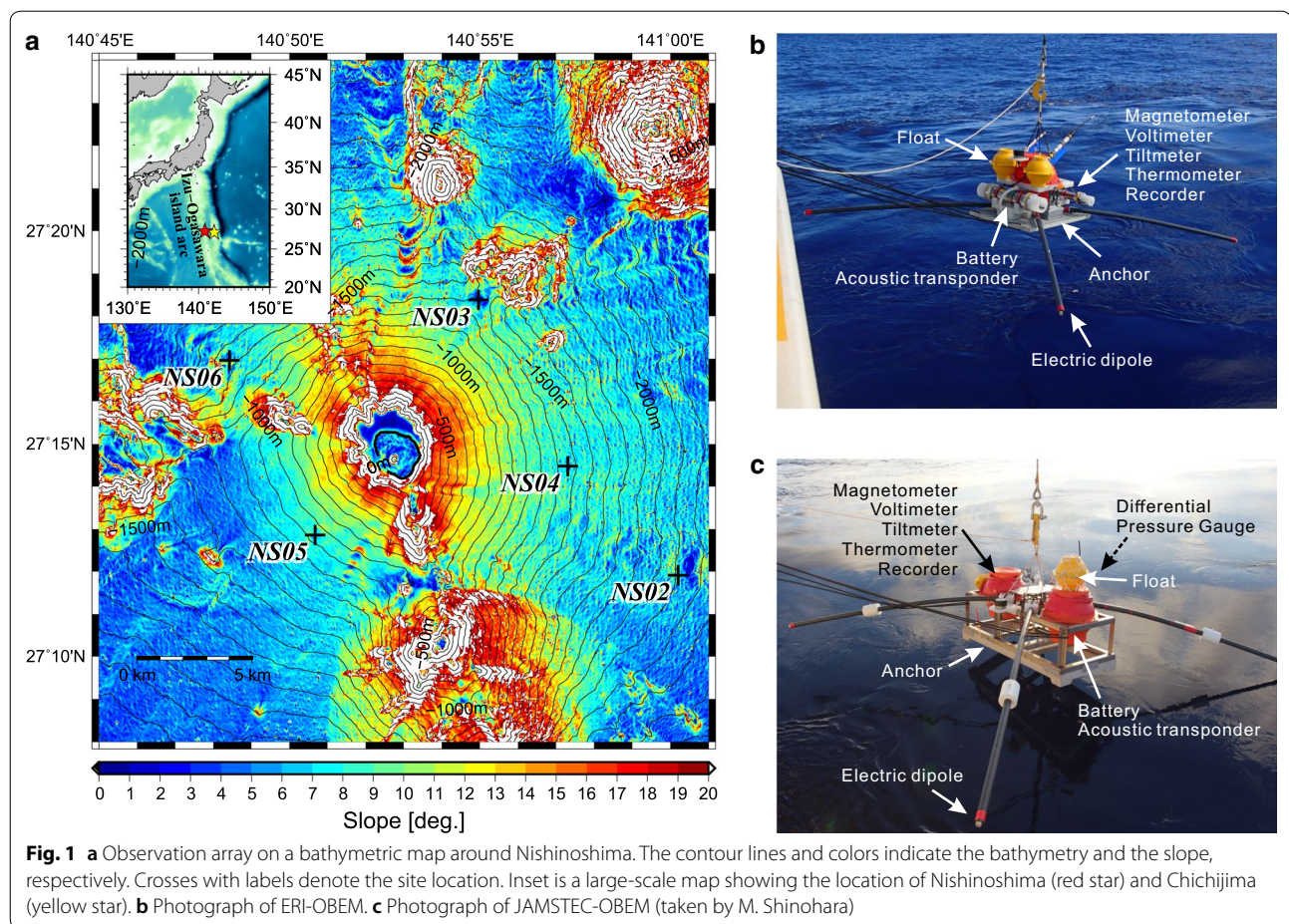
Introduction

Nishinoshima is a volcanic island in the Ogasawara (Bonin) island arc located approximately 1000 km south of Tokyo, Japan (Fig. 1a). The Nishinoshima volcano provides a unique opportunity to study island-forming eruption processes (e.g., Maeno et al. 2016; Shinohara et al. 2017; Takagi et al. 2017; Kaneko et al. 2019). The island has attracted the attention of geological researchers due to the development process of the continental crust associated with the subduction of the Pacific plate (e.g., Sano et al. 2016; Tamura et al. 2019). After an absence of nearly 40 years, eruption activity has occurred since November 2013. Seafloor seismic observations showed numerous events associated with the surface activity of the volcano, which mostly ceased in November 2015 and became active again in May 2017 (Shinohara et al. 2017). Active and quiet periods have alternated until the present time (April 2020). Maeno et al. (2016) estimated that the total volume of erupted material reached ~ 0.1 km³ and since

*Correspondence: kbaba@eri.u-tokyo.ac.jp
[1] Earthquake Research Institute, The University of Tokyo, 1-1-1, Yayoi, Bunkyo-Ku, Tokyo 113-0032, Japan
Full list of author information is available at the end of the article

Baba *et al. Earth, Planets and Space* (2020) 72:112

Page 2 of 11

Fig. 1 **a** Observation array on a bathymetric map around Nishinoshima. The contour lines and colors indicate the bathymetry and the slope, respectively. Crosses with labels denote the site location. Inset is a large-scale map showing the location of Nishinoshima (red star) and Chichijima (yellow star). **b** Photograph of ERI-OBEM. **c** Photograph of JAMSTEC-OBEM (taken by M. Shinohara)

2013, the surface area increased by $\sim 2.6 \times 10^6$ m^2 during the first 15 months of the activity.

The major component of Nishinoshima lava is andesitic (Maeno et al. 2016; Sano et al. 2016; Tamura et al. 2019), which is a critical constituent of the continental crust. From an analysis of submarine lava samples, Tamura et al. (2019) suggested that the Nishinoshima andesites are mantle-derived and that their origin is strongly influenced by the thin overlying crust. According to their model, the separation of andesite primary magma occurs just beneath the island arc Moho (~ 20 km depth) and olivine fractionation from primary andesite magma occurs in shallow crustal magma chambers. From a geochemical analysis of lava and air-fall scoria from Nishinoshima, Sano et al. (2016) confirmed that the magma chamber depth range should be 3–6 km. There are, however, no geophysical observations that imaged physical property structure possibly related to the magma beneath the volcano until the present time.

Electromagnetic (EM) and magnetic observations are frequently used for studying structure in terms of electrical conductivity and magnetization, respectively, beneath volcanoes (e.g., Aizawa et al. 2014) and for monitoring volcanic activity (e.g., Minami et al. 2018; Takahashi et al. 2018). From 2016, we conducted seafloor EM surveys using ocean bottom electromagnetometers (OBEMs). The investigation is ongoing, with the instruments being replaced in 2018 and 2019. It is the first seafloor EM experiment globally to target an active oceanic island volcano for investigation. The primary aim of the surveys is to image electrical conductivity structure, especially for the magma chambers beneath Nishinoshima through magnetotelluric analysis. The analysis is expected to constrain the depth extent of the magma chambers because electrical conductivity is sensitive to high-temperature anomalies and the presence of molten rock.

This paper reports on the data obtained from the first phase of the seafloor EM observation that was conducted in 2016–2017. In contrast to the original purpose of the experiment, we found distinct time variations in data of the instrumental tilt and the total magnetic force observed by the OBEMs. The variations occurred during a quiet period between recent major eruptions in 2015 and 2017. Upon examining the data, we are confident

Baba *et al. Earth, Planets and Space* (2020) 72:112

Page 3 of 11

that the variations are likely to be a volcanic event, as illustrated in the following sections. The investigation of the electrical structure beneath the volcano will be conducted after the additional data acquisition is completed and will be presented at a later date.

Observations and data

In this study, we utilized five OBEMs that were equipped with a three-component fluxgate magnetometer and mutually orthogonal electric dipoles to measure the time variation of the vector geomagnetic field and two horizontal components of the geoelectric field. The OBEMs were also equipped with a two-component tiltmeter and a thermometer for the correction of the attitude and the magnetic field variations, respectively, as necessary. Four of the OBEMs were supplied by the Earthquake Research Institute (ERI), The University of Tokyo. The remaining OBEM was supplied by the Japan Agency for Marine-Earth Science and Technology (JAMSTEC). We hereafter refer to them as ERI-OBEMs and JAMSTEC-OBEM.

The ERI-OBEMs and JAMSTEC-OBEM were produced by Tierra Tecnica Co. Ltd., but the specifications differ. The ERI-OBEMs are more compact in size than the JAMSTEC-OBEM, consisting of 4.6-m-long electric dipoles, glass spheres as floats, and titanium pressure cases for housing the magnetometer, acoustic transponder, and batteries (Fig. 1b). The JAMSTEC-OBEM consists of 5.4-m-long electric dipoles, two glass spheres for housing on a titanium frame, and a differential pressure gauge (Fig. 1c), which can also be used for monitoring tsunamis (Suetsugu et al. 2012; Sugioka et al. 2014). The ERI-OBEMs and JAMSTEC-OBEM share the same measurement resolution of each sensor, being 0.1 pT for the magnetometer, 1.2 nV for the voltmeter, 10^{-5} arc-degrees for the tiltmeter, and 10^{-4}°C for the thermometer. The effective resolutions in the real data are approximately 100–1000 times more than the above values because of instrumental and environmental noise.

The OBEMs were deployed on the seafloor around Nishinoshima in October 2016 and all were successfully recovered in May 2017. The observation array is shown in Fig. 1a. The ERI-OBEMs were deployed on the underwater flank of Nishinoshima where the water depth was 960–1456 m (NS03–NS06). The measurement was conducted with 8-Hz sampling intervals for 41–57 days from October 19th, 2016 until the battery was exhausted. The JAMSTEC-OBEM was deployed on the relatively deeper (2115 m) eastern flank of Nishinoshima (NS02). The sampling interval was 60 s and the data were collected for the entire observation period until the recovery. Further details of the observation sites are shown in Additional file 1: Table S1.

In this study, we focused on the magnetic field and instrumental tilt observed by the OBEMs, although the geoelectric field data were also recorded. The time series data at NS04 are shown in Fig. 2 and the same plots for the other sites are provided in Additional file 1: Figs. S1–S4. The ERI-OBEMs data were resampled every 60 s by taking a running mean of the 60 s time window. We denote x', y', and z' as mutually orthogonal directions of the observation coordinate (right-hand) system. z' directs nearly vertically down but the directions of x' and y' are not under control because the OBEM is deployed by free fall from the sea surface. The two components of the instrumental tilt, θ_{pitch} and θ_{roll} are defined as the clockwise rotation angles of $z'-x'$ plane to y' axis and $y'-z'$ plane to x' axis, respectively. The tilt data are mostly stable except during the period between November 13th and 19th (hereafter, this observation period is referred to as Period A). The three components of the magnetic field mostly changed in Period A. These observations indicate that the OBEM attitude changed. Similar changes in the tilt and the magnetic field were observed in the same time period for the other sites (Additional file 1: Figs. S1–S4). The question becomes whether the variations occurred because of the movement of the instruments only, or because of the fluctuation of the volcanic edifice. We investigate these variations further in the following sections.

Analysis and results

We converted the three components of the magnetic field data from the observation coordinate system into the geographical coordinate system (x, y, and z are the geographical north, east, and the vertical down, respectively). First, the instrumental tilt was corrected by Euler rotations of $-\theta_{\text{pitch}}$ and $-\theta_{\text{roll}}$ to reconstruct the vertical component, B_z. We denote the coordinate system at this stage by x'', y'', and $z'' (\approx z)$. $B_{x''}$, $B_{y''}$, and $B_{z''} (\approx B_z)$ at each site are shown in Fig. 2 and Additional file 1: Figs. S1–S4. The large change in the three components of the magnetic field during Period A was significantly reduced by the tilt correction. Then, the azimuthal rotation angle, $\theta_{azimuth}$, was determined to reconstruct B_x and B_y by the following equation:

$$\theta_{\text{azimuth}} = \tan^{-1}\left\{\frac{\text{median}\left(B_{y''}^{\text{quiet}}\right)}{\text{median}\left(B_{x''}^{\text{quiet}}\right)}\right\} + D_{\text{IGRF}}, \quad (1)$$

where $B_{x''}^{\text{quiet}}$ and $B_{y''}^{\text{quiet}}$ are the horizontal magnetic field components in the periods that the geomagnetic disturbance is relatively weak as Ap index is less than five and D_{IGRF} is the declination at the site predicted by the 12th

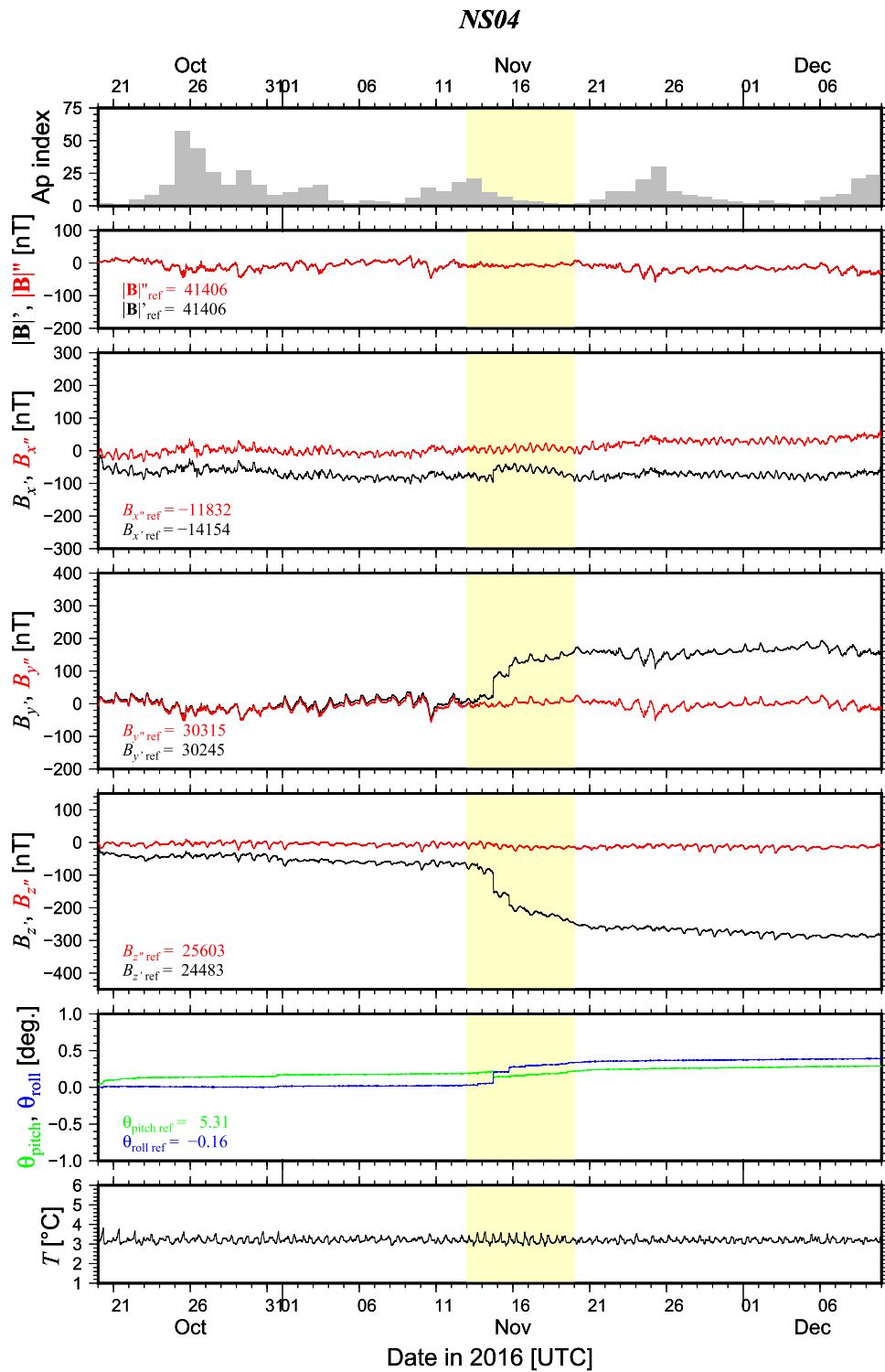Baba *et al. Earth, Planets and Space* (2020) 72:112

Page 4 of 11

Fig. 2 Time series of Ap index (top) and the data observed by the OBEM deployed at NS04. For the magnetic field data in the second to fifth rows, the black and red lines are the data before and after tilt correction, respectively. These magnetic field data and two components of the tilt data in the sixth row were shifted by a reference value indicated in each panel. The reference values are those at 00:00:00 on October 20th, 2016 (UTC). The bottom row shows the temperature measured near the fluxgate sensor. Yellow shades indicate Period A (November 13–19th, 2016). See also Additional file 1: Figs. S1–S4 for details on the other sites

Baba *et al. Earth, Planets and Space* (2020) 72:112

Page 5 of 11

Table 1 Estimation of the horizontal rotation angle, θ_{azimuth}, to convert the coordinate system into a geographical one

Site	Rotation angle (arc-degrees)		
	Before Period A	After Period A	Entire observation period
NS02	− 105.85	− 105.76	− 105.79
NS03	137.18	137.39	137.21
NS04	111.33	111.27	111.31
NS05	175.59	175.71	175.70
NS06	64.40	58.81	64.36

generation of International Geomagnetic Reference Field (IGRF) model (Thébault et al. 2015).

θ_{azimuth} was estimated for three observation periods: before Period A, after Period A, and the entire observation period. The results are listed in Table 1. For most of the sites, the estimations agree within 0.2 arc-degrees in the three observation periods. The only exception is NS06, whereby the difference in θ_{azimuth} between the before and after Period A is a significantly large 5.6 arc-degrees. The time series data for NS06 shows a large step-like change in θ_{pitch} and θ_{roll} on November 13th. The three components of the magnetic field also show a large step at the same time and the step remains after the tilt correction (see **B**′ and **B**″ in Additional file 1: Fig. S4). These results suggest that the OBEMs at NS02–NS05 were stably settled on the seafloor but the OBEM at NS06 moved.

We demonstrate the tilt of each OBEM as the $z′$ axis direction projected to the horizontal plane (Fig. 3). θ_{pitch} and θ_{roll} are plotted in the $x″$–$y″$ coordinate system. The absolute tilt angle of each OBEM is consistent with the slope of the bathymetry at each site (Fig. 1a) and the azimuth of $z′$ axis is nearly perpendicular to the bathymetric contour lines, indicating that the OBEMs were settled mostly normal to the seafloor. The instrumental tilt indicates the slope of the bathymetry resolved by 50 m mesh data based on multi-beam echo soundings.

Figure 3 shows visually how the tilt of the OBEM changed over the time at each site. The most significant change was observed at NS03. The $z′$ axis direction changed more than 1 degree to the northwest (N53° W) and in particular, it changed approximately 0.66 arc-degrees during one week in Period A. The tilt change at NS04 is complicated. It changed approximately 0.31 arc-degrees to the southeast (N163° E) during Period A, but changed slightly to the southwest before and after Period A. The tilt changes during Period A at NS02 and NS05 are smaller than those at NS03 and NS04, being 0.14

arc-degrees to the east (N91° E) and 0.12 arc-degrees to the west (N84° W), respectively. For NS06, the tilt jumped on November 13th but this is likely to have been caused by the movement of the OBEM on the seafloor, as demonstrated above.
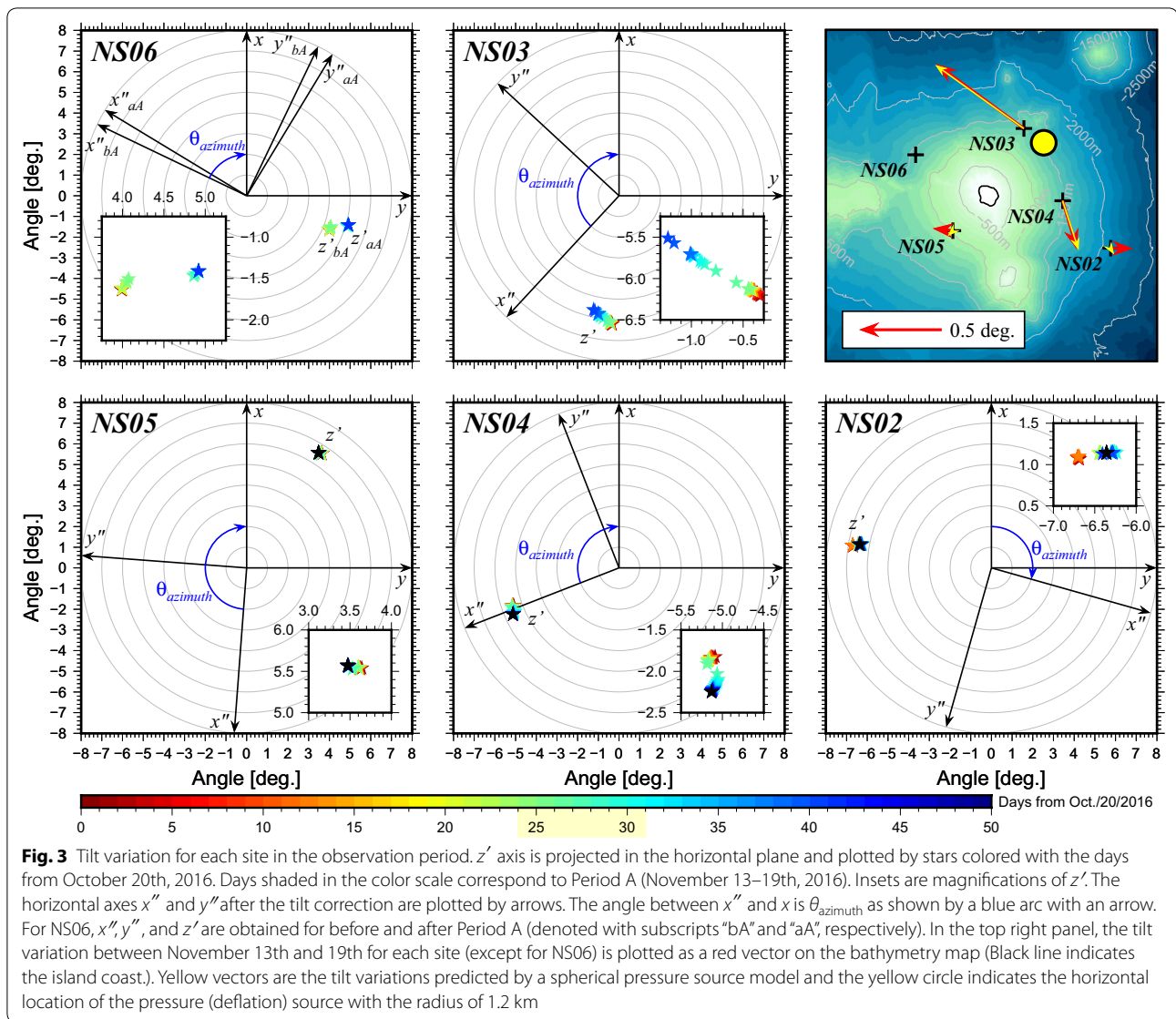
We should note that the observed tilt variations might include a certain degree of local (site-dependent) responses. The OBEMs were deployed by free fall from the sea surface and therefore, it is not guaranteed that they were coupled to the seafloor with adequate strength. The angle between the seafloor and the OBEM may be changed by an external force triggered by the regional event. Three observations lead us to suspect the possibility of mixing with local responses. First, the tilt variations during Period A include step-like abrupt changes and these steps are not coincident between the sites. Second, the tilt variation is more significant for the rolling angle than for the pitching angle at NS03, NS04, NS05, and NS06, which are all records by the ERI-OBEMs (Figs. 2, 3, and Additional file 1: Figs. S2–S4.), suggesting the possibility of an instrumental response. For ERI-OBEMs, the pressure case housing the tilt sensors is separated more from the instrument gravity center in the $y′$-direction than in $x′$-direction and therefore, the rolling angle can be changed by a smaller force than that required to change the pitching angle. Third, the observed tilt variations of 0.12–0.66 arc-degrees/week (order of 10^{-4}–10^{-3} radians/day) are very large compared to the reported tilt variations for other volcanoes, which may be at a maximum of 10^{-4} radians/day (e.g., Gambino et al. 2014).

Next, we synthesized the total magnetic force from the data of the three components. The total magnetic force is the absolute value of the vector magnetic field,

$$|\mathbf{B}| = \sqrt{B_x^2 + B_y^2 + B_z^2}. \tag{2}$$

$|\mathbf{B}|$ is independent from the instrumental attitude by its definition and it is invariant to the coordinate system rotation. We calculated the total magnetic forces $|\mathbf{B}|′$ and $|\mathbf{B}|″$ from the three components of the magnetic field data for the original observation coordinate system ($B_{x′}$, $B_{y′}$, and $B_{z′}$) and for the coordinate system after the instrumental tilt correction ($B_{x″}$, $B_{y″}$, and $B_{z″}$), respectively (Fig. 2 and Additional file 1: Figs. S1–S4). They should be identical if the vector magnetic field is correctly measured, i.e., $|\mathbf{B}| = |\mathbf{B}|′ = |\mathbf{B}|″$. In Fig. 2 and Additional file 1: Figs. S1–S4, the difference between $|\mathbf{B}|′$ and $|\mathbf{B}|″$ is invisible. The root mean square (RMS) of $|\mathbf{B}|′ − |\mathbf{B}|″$ was less than 0.1 nT for all sites.

We further calculated the residuals of the total magnetic force to a reference site to reduce the effects of the external geomagnetic fluctuations. We used the total magnetic force data collected at the Chichijima

Fig. 3 Tilt variation for each site in the observation period. z' axis is projected in the horizontal plane and plotted by stars colored with the days from October 20th, 2016. Days shaded in the color scale correspond to Period A (November 13–19th, 2016). Insets are magnifications of z'. The horizontal axes x'' and y'' after the tilt correction are plotted by arrows. The angle between x'' and x is $\theta_{azimuth}$ as shown by a blue arc with an arrow. For NS06, x'', y'', and z' are obtained for before and after Period A (denoted with subscripts "bA" and "aA", respectively). In the top right panel, the tilt variation between November 13th and 19th for each site (except for NS06) is plotted as a red vector on the bathymetry map (Black line indicates the island coast.). Yellow vectors are the tilt variations predicted by a spherical pressure source model and the yellow circle indicates the horizontal location of the pressure (deflation) source with the radius of 1.2 km

geomagnetic observatory (CBI), which is located approximately 130 km east of Nishinoshima (Fig. 4a). The residuals indicate a decreasing trend for NS03, NS04, NS05, and NS06, the data of which were obtained by the ERI-OBEMs. However, no significant trend is observed for NS02, the data of which were obtained by the JAMSTEC-OBEM. We suspect that the trend is probably due to an instrumental systematic problem, previously experienced. We applied a low pass filter with the cut-off period of 48 h to the residual data, with the exception of NS06–CBI because the NS06 data jumped on November 13th. We further removed a linear trend that fitted the data before Period A in a least square sense. The trends are similar (3.0 ~ 3.7 nT/week) between the residuals for NS03, NS04, and NS05, where it is 0.3 nT/week for NS02. The results illustrate

a clear change in the total magnetic force residuals that coincide with tilt changes during Period A. Once again, these are more significant for NS03 ($+ 9.1 \pm 0.3$ nT) and NS04 ($- 7.6 \pm 0.3$ nT) compared to the changes for NS02 ($+ 1.5 \pm 0.3$ nT) and NS05 ($+ 0.2 \pm 0.4$ nT).

The results are considered reliable, although the total magnetic force synthesized from the data of the three components may be uncertain compared with direct measurement such as using a proton precession magnetometer. The uncertainty can be mainly derived from the following two points: (1) the magnetic field data measured by fluxgate sensor drifts with temperature variation and (2) inaccuracy of the mutual orthogonality between the three-component sensors may affect the synthesized total force variation. If it is not adequately accurate, the synthesized total force is not independent
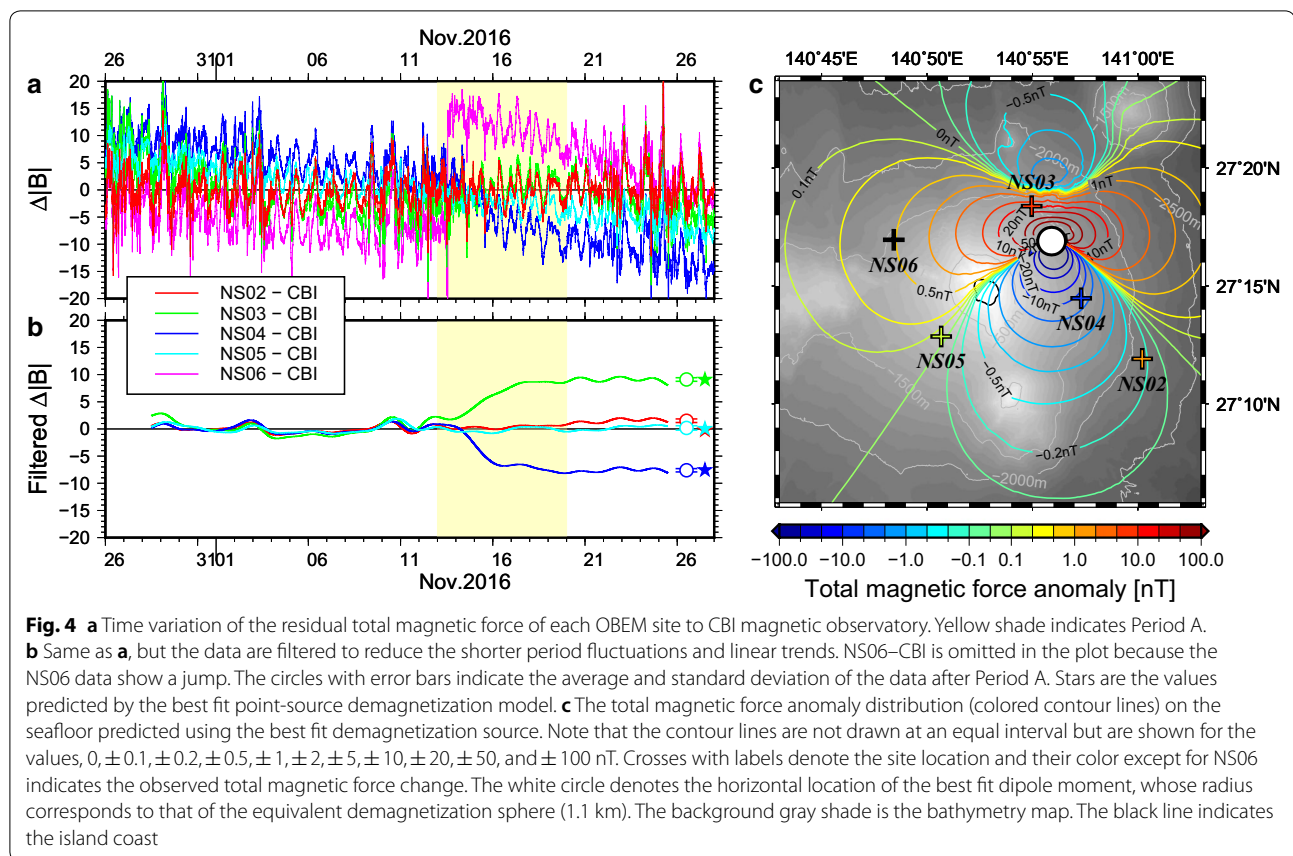
Baba *et al. Earth, Planets and Space*   (2020) 72:112

Page 7 of 11

Fig. 4 **a** Time variation of the residual total magnetic force of each OBEM site to CBI magnetic observatory. Yellow shade indicates Period A. **b** Same as **a**, but the data are filtered to reduce the shorter period fluctuations and linear trends. NS06–CBI is omitted in the plot because the NS06 data show a jump. The circles with error bars indicate the average and standard deviation of the data after Period A. Stars are the values predicted by the best fit point-source demagnetization model. **c** The total magnetic force anomaly distribution (colored contour lines) on the seafloor predicted using the best fit demagnetization source. Note that the contour lines are not drawn at an equal interval but are shown for the values, $0, \pm 0.1, \pm 0.2, \pm 0.5, \pm 1, \pm 2, \pm 5, \pm 10, \pm 20, \pm 50$, and ± 100 nT. Crosses with labels denote the site location and their color except for NS06 indicates the observed total magnetic force change. The white circle denotes the horizontal location of the best fit dipole moment, whose radius corresponds to that of the equivalent demagnetization sphere (1.1 km). The background gray shade is the bathymetry map. The black line indicates the island coast

of the tilt variation. The temperature is quite stable during the entire observation periods for all sites, although we can observe daily variations, which are as large as approximately 1.5 °C at the shallowest site NS05 and as small as approximately 0.3 °C at the deepest site NS02 (Fig. 2 and Additional file 1: Figs. S1–S4). There is no visible change in the temperature correlated with the tilt change during Period A. According to the maker catalog, the drift of the fluxgate magnetometer is 0.2 nT/ °C and therefore, the temperature variation did not cause a significant change in the total force residuals during Period A. The mutual orthogonality of the three-component sensors was tested during the instrument production process by comparing the synthesized total force with reference data at a geomagnetic observatory. The standard deviation of the residuals was typically less than 2 nT for the ERI-OBEMs and JAMSTEC-OBEM, which is again smaller than the variation in the total force residual we observed during Period A. The slight difference between $|\mathbf{B}|'$ and $|\mathbf{B}|''$ as demonstrated above, also suggests that the mutual orthogonality is adequately accurate for the current discussion.

Our analyses and examinations lead us to conclude that the instrumental tilt and geomagnetic total force, which

are mutually independent, varied significantly around the same time during Period A. The coincidence of the two independent data variations between the sites was not artificial but real, which could be associated with a volcanic (but non-eruptive) event beneath the Nishinoshima volcanic edifice.

Discussion

We attempted to investigate the physical processes behind the observed variations, although providing a thorough interpretation from the data at only four available observation sites was a limiting factor. There are many reports regarding the change in the geomagnetic field around and deformation of, a volcanic edifice, which are frequently interpreted by thermal demagnetization and inflation of the volcanic edifice, respectively, due to ascending hot magma (e.g., Hotta and Iguchi, 2017; Takahashi et al. 2018). Our data show that both the total magnetic force and tilt variations during Period A were more significant at sites NS03 and NS04. These observations suggest that a source of these variations would be located somewhere between the two sites. In this study, we investigated whether the data are explained consistently by simple magnetic and pressure source models.

Baba *et al. Earth, Planets and Space* (2020) 72:112

Page 8 of 11

The total magnetic force variation is positive for the northern site, NS03, and negative for the southern site, NS04. This trend is qualitatively consistent with the anomaly caused by demagnetization of the crust between the two sites under the ambient geomagnetic field of the northern hemisphere. We inverted the total magnetic force difference between the periods before and after Period A at the four sites and estimated a single magnetic dipole moment intensity and its location, assuming that the moment is parallel to the ambient geomagnetic field represented by IGRF (37.4 and -4.3 arc-degrees for the inclination and declination, respectively). The best fit magnetic dipole moment intensity and its location were obtained by a grid search method and they are -9.1×10^9 Am^2 and 27°16.90′ N, 140°55.91′ E, 2600 m below sea surface ($\sim$1200 m below the seafloor), respectively (Fig. 4c), where negative value for the moment intensity means demagnetization. This solution predicts well the observed total magnetic force changes, although the misfit for NS02 is relatively large (Fig. 4b, c). The absolute magnetic dipole moment intensity is large compared to estimates for other volcanoes in Japan (Hashimoto et al. 2019). This suggests that this event may be significantly large in terms of volcanic activity in island arcs and/or governed by more complex underlying mechanisms that are discussed below. Although our data cannot provide information regarding where the heat for the demagnetization comes from, it is notable that the estimated demagnetization source depth is comparable to the top depth of the magma chamber estimated by Sano et al. (2016). This might suggest that the magma just beneath Nishinoshima Island moved laterally to the northeast. A similar mechanism was proposed for another volcanic island, Miyakejima that was active in 2000 (e.g., Furuya et al. 2003).

The volume of the demagnetization zone may be estimated from the dipole moment intensity and magnetization. The average magnetization of the Nishinoshima volcano body was estimated to be approximately 1.7 Am^{-1} (Iizuka et al. 1975). This estimate was obtained from a geomagnetic survey after eruptions that occurred more than 40 years ago. Although the fresh and thus possibly more strongly magnetized lava from the recent eruptions since 2013 partly covered the old volcano body, the estimate should be a good approximation of at least the lower bound. Assuming 1.7 Am^{-1} for the average magnetization of the volcano body, the volume of demagnetized zone is estimated to be 5.3 km^3, of which the radius is 1.1 km if a spherical zone is assumed. The radius is slightly smaller than the source depth below the seafloor, suggesting that the heat causing the demagnetization would have reached close to the seafloor. However, in November 2016, neither eruptions on the island were

reported nor seismic signals observed by ocean bottom seismometers were not significantly increased (Shinohara et al. 2017).

These results may be attributed to three possibilities, (1) the average magnetization is greater than the assumed value, 1.7 Am^{-1}, (2) the demagnetization zone is not a spherical shape, and/or (3) other unknown processes. For (1), doubling the average magnetization would yield an estimated 21% reduction in the radius of the sphere. For (2), the source may be deeper and smaller in its volume with greater complex geometry. However, it is difficult to quantitatively consider the complex geometry based on the existing limited data on the total magnetic force anomaly. The ratio of the demagnetization zone radius to the distance from the nearest site (NS03) is approximately 0.3. In a similar case, Kanda et al. (2010) pointed out that observed magnetic changes could not be attributed to a spherical demagnetization source, and instead investigated triaxial ellipsoid sources. The vector magnetic component data may be useful to discuss source geometry of greater complexity. However, the reliability of this data is secondary because there is no guaranteed independence of the vector magnetic component data from the tilt data. Inversion of the vector data assuming a rectangular prism as a demagnetization source suggests the potential for NE-oriented vertical sheet-like geometry in the similar horizontal location with but in greater depth than the source determined by the total magnetic force anomaly data (see Additional file 2).

The magnetization phase due to cooling should follow the demagnetization phase, however, the available data length after Period A is probably too short to discuss such a process (Fig. 4b).

The tilt variation observed by the OBEMs can provide information regarding volcanic edifice deformation, although the quantitative interpretation is not straightforward. The coincidental tilt variations during Period A, which are particularly significant for NS03 and NS04 and similar to the total magnetic force variations, suggests that the tilt variations can be attributed to a volcanic unrest event. The z'-axis projected on the horizontal plane moved to the northwest for NS03 and to the southeast for NS04 (Fig. 3), meaning that the tilts varied to depress the seafloor between the two sites. However, we cannot rule out that the observed tilt variations include local responses as mentioned in the previous section.

We estimated the volume change and its location to explain the observed tilt differences between the before and after Period A at the four sites (except for NS06), assuming an isotropic spherical pressure source (Mogi 1958). Here, we assumed that the observed tilt variations are caused only by the single pressure source in homogeneous media, ignoring the possibility of mixing with

Baba *et al. Earth, Planets and Space*   (2020) 72:112

Page 9 of 11

local responses. The volume change of -7.9 km^3, the source location of 27°17.61′ N, 140°56.16′ E, and 6600 m below sea surface (approximately 5100 m below sea floor) were obtained as the best fit parameters by a grid search method. The model obtained better predicts both magnitude and direction of the observed tilt changes at NS03 and NS04, but does not predict the observations for NS02 and NS04 very well (Fig. 3). This is because the model can only produce axially symmetric deformation to the source. The horizontal location of the pressure source is close to that of the demagnetization source, but the depth is much larger. The negative volume change means a deflation of the volcanic edifice. The volume change obtained is much more significant than the estimations for other volcanic activities in Japan (e.g., Furuya et al. 2003; Hashimoto et al. 2019) and the result is inconsistent with the typical ascending magma scenario whereby the magma intrusion inflates the volcanic edifice and the heat from the magma demagnetizes the volcanic body.

This inconsistency may be due to the simple model setting for the magnetic and pressure sources, in addition to neglecting possible local responses in the observed tilt variations. The ratio between the radius of the spherical volume change and the pressure source depth was approximately 0.24, suggesting that the radius is too large to hold the spherical source approximation (e.g., Sakai et al. 2007). From observations of Sicilian volcanoes, Gambino et al. (2014) postulated that dike intrusions can cause variations in larger tilt in shorter durations (several hours to a few days) than inflation/deflation of volcanic edifice (several weeks to years). The duration of Period A is comparable with that of dike intrusions. Deformation due to dike intrusion is not axial symmetry and the tilt can vary to depress the seafloor in the vicinity of the dike (e.g., Okada 1985). Pressure source depth would be overestimated if a spherical source model is applied to dike-type deformation (Seismology and Volcanology Research Department MRI 2013). Additionally, the magnetic source may be a dike-like vertical sheet elongated in the NE direction. It may also be deeper than estimated from the total magnetic force anomaly data as the analysis using vector magnetic data suggested (Additional file 2), although agreement is not necessary. However, the lack of observed significant seismicity in Period A (Shinohara et al. 2017) is difficult to understand, as significant seismicity associated with dike intrusions was observed in the Miyakejima volcano (Ueda et al. 2006). As Shinohara et al. (2017) focused on high frequency (4–8 Hz) events associated with eruptions at Nishinoshima creator, the possibility that low frequency events occurred in Period A cannot be ruled out. The volcano topography is not considered in our calculations, although the tilt data can be affected by the topography (e.g., Sakai et al. 2007;

Marsden et al. 2019). The current limited data set is not suitable for considering such complexities quantitatively and therefore we leave for further discussion. Accumulation of various observations is indispensable to understand this kind of interesting volcanic activities more deeply.

This study showed that the OBEMs, especially for the magnetic field observations, are useful to monitor and study activities of island volcanoes, although the instruments and the observations reported here were not ideally designed for such purposes. The OBEMs measure the time variation of the magnetic and electric fields and instrumental tilts by a single system so that they can provide some independent information on volcanic activity. In this study, we demonstrated the possibility of changes in the magnetization structure and the deformation of the volcanic edifice. There are other potential possibilities that we have not studied. The time variation in the electrical conductivity structure may be detected by magnetotelluric analysis using the electric and magnetic field data if enough data are observed.

To strengthen the usefulness of OBEMs, more strategic observations would be important. Larger, denser, and longer array observations would be necessary to constrain realistic activity sources and their locations and temporal variations. The estimation of the OBEM position on the seafloor is more important for observations around active volcanoes than observations on stable seafloors. The OBEM at NS06 was thought to be moved during the observation. In this observation, the OBEM position was measured only at the deployment time. Measuring the position at both deployment and recovery times will be useful to confirm the stable settlement of OBEMs more directly. Longer continuous observations to continuously monitor the activity are critical. Although the available array data duration was only 41 days in this study, the OBEMs can measure for approximately 1 year if the amount of batteries and the sampling intervals are adjusted. Observations over years are achievable by replacing the instruments every year.

Conclusions
The Nishinoshima Island volcano was investigated by means of a marine electromagnetic method. From the data obtained by five OBEMs in the first observation phase from 2016 to 2017, we found significant variations in the geomagnetic field and tilt of the volcanic slope in the middle of November 2016, at which time no eruptions were observed. As expected theoretically, we confirmed the independency of the total magnetic force synthesized from the vector magnetic field data to the instrumental attitude. The significant coincidence variations in the total magnetic force and the tilt at the sites

Baba *et al. Earth, Planets and Space*   (2020) 72:112

Page 10 of 11

and their distribution in the observation array suggest that they are caused by a volcanic process and the possible source is beneath the volcanic slope in the northeast of Nishinoshima Island. The magnetic and pressure sources were estimated assuming a simple magnetic dipole moment and spherical volume changes. The horizontal locations of the two sources were determined in the NE of the island. However, the depths are significantly different (~ 1200 and ~ 5100 m below seafloor for the magnetic and pressure sources, respectively), and the demagnetization volume (5.3 km^3) and deflation volume (7.9 km^3) were too large to maintain the simple source assumptions. Whilst there should be consideration given to source geometry and mechanisms of greater complexity, such as dike intrusion, the limited available data restricted further quantitative discussion.

Our finding indicates that OBEMs are useful for monitoring the activity of volcanic islands, although the instrument and the observation around Nishinoshima were not ideally designed for such a purpose. We analyzed the magnetic field and tilt data in this study although the OBEMs measured the time variations of the electric field and also differential pressure for the JAMSTEC-OBEM. The OBEMs should have more potential for this kind of study than presented here if they are deployed strategically in terms of observation scale, density, and duration.

Supplementary information

Supplementary information accompanies this paper at https://doi.org/10.1186/s40623-020-01240-z.

Additional file 1. Site information (Table S1) and figures for the time series data observed by the OBEMs at NS02, NS03, NS05, and NS06 (Figures S1-S4).

Additional file 2. Magnetic source analysis using the horizontal and vertical field component anomalies and the results (Figures S5 and S6).

Abbreviations

EM: Electromagnetic; OBEM: Ocean bottom electromagnetometer; ERI: Earthquake Research Institute; JAMSTEC: Japan Agency for Marine-Earth Science and Technology; IGRF: International Geomagnetic Reference Field; RMS: Root mean square.

Authors' contributions

KB, NT, HS, YH, AT, and MT contributed to the seafloor EM data acquisition, joining the OBEM deployment and recovery cruises. HI and TK supported the observations before and after the cruises. KB processed the time-series data and conducted the inversion of the tilt variation data. HI conducted the inversion analysis of the total magnetic force variation data with support by TK. MT led the entire project of the Nishinoshima geophysical and geological observations, and obtained research funding. NT led the EM observations, and obtained research funding. KB wrote the manuscript. All authors read and approved the final manuscript.

Availability of data and materials

The OBEM time-series data for the magnetic field and the tilt used and/or analyzed during the current study are available from the corresponding author upon reasonable request.

Ethics approval and consent to participate

Not applicable.

Consent for publications

Not applicable.

Competing interests

The authors declare that they have no competing interests.

Author details

[1] Earthquake Research Institute, The University of Tokyo, 1-1-1, Yayoi, Bunkyo-Ku, Tokyo 113-0032, Japan. [2] Volcanoes and Earth's Interior Research Center, Research Institute for Marine Geodynamics, Japan Agency for Marine-Earth Science and Technology, 2-15 Natsushima-cho, Yokosuka, Kanagawa 237-0061, Japan. [3] Earthquake and Volcano Research Center, Graduate School of Environmental Studies, Nagoya University, D2-2, Furo-cho, Chikusa-ku, Nagoya, Aichi 464-8601, Japan. [4] Kobe Ocean-Bottom Exploration Center, Kobe University, 5-1-1, Fukaeminami-cho, Higashinada-ku, Kobe, Hyogo 658-0022, Japan. [5] Graduate School of Science, Kobe University, 1-1, Rokkodai-cho, Nada-ku, Kobe, Hyogo 657-8501, Japan. [6] Japan Meteorological Agency, 1-3-4, Otemachi, Chiyoda-ku, Tokyo 100-8122, Japan.

References

Aizawa K, Koyama T, Hase H, Uyeshima M, Kanda W, Utsugi M, Yoshimura R, Yamaya Y, Hashimoto T, Yamazaki K, Komatsu S, Watanabe A, Miyakawa K, Ogawa Y (2014) Three-dimensional resistivity structure and magma plumbing system of the Kirishima volcanoes as inferred from broadband magnetotelluric data. J Geophys Res Solid Earth 119:198–215. https://doi.org/10.1002/2013JB010682

Furuya M, Okubo S, Kimata F, Miyajima R, Meilano I, Sun W, Tanaka Y, Miyazaki T (2003) Mass budget of the magma flow in the 2000 volcano-seismic activity at Izu-islands, Japan. Earth Planets Space 55:375–385. https://doi.org/10.1186/BF03351771

Gambino S, Falzone G, Ferro A, Laudani G (2014) Volcanic processes detected by tiltmeters: a review of experience on Sicilian volcanoes. J Volcanol Geotherm Res 271:43–54. https://doi.org/10.1016/j.jvolgeores.2013.11.007

Hashimoto T, Utsugi M, Okura T, Kanda W, Terada A, Miura S, Iguchi M (2019) On the source characteristics of demagnetization and ground deformation associated with non-magmatic activity. Kazan 64(2):103–109. https://doi.org/10.18940/kazan.64.2_103 **(in Japanese with English abstract)**

Hotta K, Iguchi M (2017) Ground deformation source model at Kuchino-erabu-jima volcano during 2006–2014 as revealed by campaign GPS observation. Earth Planets Space 69:173. https://doi.org/10.1186/s40623-017-0763-7

Iizuka S, Saki T, Inokuchi H, Shinoyama Y (1975) Geophysical investigations of volcano Nishinoshima, Ogasawara (Bonin) Islands. Kazan 20(3):141–155.

https://doi.org/10.18940/kazanc.20.3_141 **(in Japanese with English abstract)**

Kanda W, Utsugi M, Tanaka Y, Hashimoto T, Fujii I, Hasenaka T, Shigeno N (2010) A heating process of Kuchi-erabu-jima volcano, Japan, as inferred from geomagnetic field variations and electrical structure. J Volcanol Geotherm Res 189:158–171. https://doi.org/10.1016/j.jvolgeores.2009.11.002

Kaneko T, Maeno F, Yasuda A, Takeo M, Takasaki K (2019) The 2017 Nishinoshima eruption: combined analysis using Himawari-8 and multiple high-resolution satellite images. Earth Planets Space 71:140. https://doi.org/10.1186/s40623-019-1121-8

Maeno F, Nakada S, Kaneko T (2016) Morphological evolution of a new volcanic islet sustained by compound lava flows. Geology 44(4):259–262. https://doi.org/10.1130/G37461.1

Marsden LH, Neuberg JW, Thomas ME (2019) Topography and tilt at volcanoes. Front Earth Sci 7:317. https://doi.org/10.3389/feart.2019.00317

Minami T, Utsugi M, Utada H, Kagiyama T, Inoue H (2018) Temporal variation in the resistivity structure of the first Nakadake crater, Aso volcano, japan, during the magmatic eruptions from November 2014 to May 2015, as inferred by the ACTIVE electromagnetic monitoring system. Earth Planets Space 70:138. https://doi.org/10.1186/s40623-018-0909-2

Mogi K (1958) Relations between the eruptions of various volcanoes and the deformations of the ground surface around them. Bull Earthq Res Inst Univ Tokyo 36:99–134. http://hdl.handle.net/2261/11909

Okada Y (1985) Surface deformation due to shear and tensile faults in a half-space. Bull Seismol Soc Am 75:1135–1154

Sakai T, Yamamoto T, Fukui K, Fujiwara K, Takagi A, Churei M (2007) Establishment of precision of calculation for volcanic crustal deformation by FEM. Pap Meteorol Geophys 58:1–15. https://doi.org/10.2467/mripapers.58.1

Sano T, Shirao M, Tani K, Tsutsumi Y, Kiyokawa S, Fujii T (2016) Progressive enrichment of arc magmas caused by the subduction of seamounts under Nishinoshima volcano, Izu-Bonin Arc, Japan. J Volcanol Getherm Res 319:52–65. https://doi.org/10.1016/j.jvolgeores.2016.03.004

Seismology and Volcanology Research Department MRI (2013) Development of quantitative detection techniques of magma activity and improvement of evaluation of volcanic activity level. Tech Rep Meteorol Res Inst 69: 179. https://doi.org/10.11483/mritechrepo.69 **(in Japanese with English abstract)**

Shinohara M, Ichihara M, Sakai S, Yamada T, Takeo M, Sugioka H, Nagaoka Y, Takagi A, Morishita T, Ono T, Nishizawa A (2017) Continuous seismic monitoring of Nishinoshima volcano, Izu Ogasawara, by using long-term ocean bottom seismometers. Earth Planets Space 69:159. https://doi.org/10.1186/s40623-017-0747-7

Suetsugu D, Shiobara H, Sugioka H, Ito A, Isse T, Kasaya T, Tada N, Baba K, Abe N, Hamano Y, Tarits P, Barriot JP, Reymond D (2012) TIARES Project—Tomographic investigation by seafloor array experiment for the Society hot-spot. Earth Planets Space 64:i–iv. https://doi.org/10.5047/eps.2011.11.002

Sugioka H, Hamano Y, Baba K, Kasaya T, Tada N, Suetsugu D (2014) Tsunami: ocean dynamo generator. Sci Rep 4:3596. https://doi.org/10.1038/srep03596

Takagi A, Nagaoka Y, Fukui K, Ando S, Kimura K, Tsuchiyama H (2017) Studies on monitoring of the 2013–1015 Nishinoshima eruption. Tech Rep Meteorol Res Inst 78:72. https://doi.org/10.11483/mritechrepo.78

Takahashi K, Takakura S, Matsushima N, Fujii I (2018) Relationship between volcanic activity and shallow hydrothermal system at Mekandake volcano, Japan, inferred from geomagnetic and audio-frequency magnetotelluric measurements. J Volcanol Geotherm Res 349:351–369. https://doi.org/10.1016/j.jvolgeores.2017.11.019

Tamura Y, Ishizuka O, Sato T, Nichols ARL (2019) Nishinoshima volcano in the Ogasawara Arc: new continent from the ocean? Island Arc. 28(1):e12285. https://doi.org/10.1111/iar.12285

Thébault E, Finlay CC, Beggan CD, Alken P, Aubert J, Barrois O, Bertrand F, Bondar T, Boness A, Brocco L, Canet E, Chambodut A, Chulliat A, Coïsson P, Civet F, Du A, Fournier A, Fratter I, Gillet N, Hamilton B, Hamoudi M, Hulot G, Jager T, Korte M, Kuang W, Lalanne X, Langlais B, Léger J-M, Lesur V, Lowes FJ, Macmillan S, Mandea M, Manoj C, Maus S, Olsen N, Petrov V, Ridley V, Rother M, Sabaka T-J, Saturnino D, Schachtschneider R, Sirol O, Tangborn A, Thomson A, Lars T-C, Vigneron P, Wardinski I, Zvereva T (2015) International Geomagnetic Reference Field: the 12th generation. Earth Planets Space 67:79. https://doi.org/10.1186/s40623-015-0228-9

Ueda H, Matsumoto T, Fujita E, Ukawa M, Yamamoto E, Sasai Y, Irwan M, Kimata F (2006) Geomagnetic changes associated with dike intrusion during the 2000 Miyakejima eruptive activity, Japan. Earth Planet Sci Lett 245:416–426. https://doi.org/10.1016/j.epsl.2006.02.036

Wessel P, Smith WHF, Scharroo R, Luis J, Wobbe F (2013) Generic mapping tools: improved version released. Eos Trans AGU 94(45):409–410. https://doi.org/10.1002/2013EO450001

Publisher's Note

Springer Nature remains neutral with regard to jurisdictional claims in published maps and institutional affiliations.